



Haplotype-Based Analysis of *KIR*-Gene Profiles in a South European Population—Distribution of Standard and Variant Haplotypes, and Identification of Novel Recombinant Structures

Elisa Cisneros¹, Manuela Moraru¹, Natalia Gómez-Lozano¹, Aura Muntasell², Miguel López-Botet^{2,3} and Carlos Vilches^{1*}

¹ Immunogenetics and Histocompatibility, Instituto de Investigación Sanitaria Puerta de Hierro Segovia de Arana, Madrid, Spain, ² Hospital del Mar Medical Research Institute (IMIM), Barcelona, Spain, ³ Department of Experimental and Health Sciences, University Pompeu Fabra, Barcelona, Spain

OPEN ACCESS

Edited by:

Martin Maiers,
National Marrow Donor Program,
United States

Reviewed by:

Karl-Johan Malmberg,
Oslo University Hospital, Norway
Francesco Colucci,
University of Cambridge,
United Kingdom

*Correspondence:

Carlos Vilches
carlos.vilches@yahoo.com

Specialty section:

This article was submitted to
NK and Innate Lymphoid Cell Biology,
a section of the journal
Frontiers in Immunology

Received: 19 January 2020

Accepted: 26 February 2020

Published: 17 March 2020

Citation:

Cisneros E, Moraru M, Gómez-Lozano N, Muntasell A, López-Botet M and Vilches C (2020) Haplotype-Based Analysis of *KIR*-Gene Profiles in a South European Population—Distribution of Standard and Variant Haplotypes, and Identification of Novel Recombinant Structures. *Front. Immunol.* 11:440. doi: 10.3389/fimmu.2020.00440

Inhibitory Killer-cell Immunoglobulin-like Receptors (KIR) specific for HLA class I molecules enable human natural killer cells to monitor altered antigen presentation in pathogen-infected and tumor cells. *KIR* genes display extensive copy-number variation and allelic polymorphism. They organize in a series of variable arrangements, designated *KIR* haplotypes, which derive from duplications of ancestral genes and sequence diversification through point mutation and unequal crossing-over events. Genomic studies have established the organization of multiple *KIR* haplotypes—many of them are fixed in most human populations, whereas variants of those have less certain distributions. Whilst *KIR*-gene diversity of many populations and ethnicities has been explored superficially (frequencies of individual genes and presence/absence profiles), less abundant are in-depth analyses of how such diversity emerges from *KIR*-haplotype structures. We characterize here the genetic diversity of KIR in a sample of 414 Spanish individuals. Using a parsimonious approach, we manage to explain all 38 observed *KIR*-gene profiles by homo- or heterozygous combinations of six fixed centromeric and telomeric motifs; of six variant gene arrangements characterized previously by us and others; and of two novel haplotypes never detected before in Caucasoids. Associated to the latter haplotypes, we also identified the novel transcribed *KIR2DL5B*0020202* allele, and a chimeric *KIR2DS2/KIR2DL3* gene (designated *KIR2DL3*033*) that challenges current criteria for classification and nomenclature of *KIR* genes and haplotypes.

Keywords: copy-number variation, genes, haplotypes, KIR, NK cells, polymorphism

INTRODUCTION

Human killer-cell immunoglobulin-like receptors (KIR) are a diverse and polymorphic family of glycoproteins that convey inhibitory or activating signals to subpopulations of NK and T lymphocytes upon recognition of their ligands, mainly HLA class I allotypes (1). In coordination with multiple other activating and inhibitory receptors for HLA class I and non-HLA molecules,

KIR regulate the function of cytotoxic lymphocytes, providing them with a capacity to sense modifications of HLA expression on potential target cells (2, 3).

KIR repertoires expressed by NK cells of different individuals display a conspicuous phenotypic and functional diversity, genetically determined in its greatest part. KIR are encoded in a ~100–250 Kbp complex on chromosome 19q13.4, where variable combinations of 15 *KIR* genes and 2 pseudogenes arrange in a head-to-tail orientation, separated by intergenic regions of only ~2.5 Kbp (4). Another ancestral gene, *KIR3DX1* (5), lays ~178 Kbp upstream of the *KIR* complex, in the middle of the *LILR-LAIR* gene cluster (Figure 1).

The *KIR* complex is extremely diverse due to allelic polymorphism and gene copy-number variation (CNV). Only three “framework” regions of the *KIR* complex are relatively well-conserved in their gene content: the genes at the 5′ and 3′ ends (*KIR 3DL3* and *3DL2*, respectively), and a central cluster formed by *KIR 3DP1* and *2DL4*. These framework *KIR* genes define the limits of two intervals, centromeric (5′) and telomeric (3′), containing variable combinations of the other genes (4, 6–10). Certain gene arrangements or “motifs” are particularly common within each of those intervals (Figure 1); in turn, the different centromeric and telomeric gene motifs are seen in any combinatorial association, possibly owing to a recombination hot-spot between *KIR 3DP1* and *2DL4*.

Restriction-fragment length polymorphism studies published in 1997 sorted *KIR* genotypes into categories “A” and “B,” based on variable presence of a 24 Kbp-long *HindIII* band, later shown to derive from the *KIR2DL5* gene (11, 12). This definition was then refined and adapted (13), so that “A haplotype” now officially designates a nearly fixed combination of seven genes and pseudogenes, encoding the HLA-C-specific *KIR 2DL3* and *2DL1* in the variable centromeric interval, and *3DL1* and *2DS4* in the telomeric one. In contrast, “B” designates collectively a vast array of haplotypes bearing any additional *KIR* gene (even when they also have, as it often happens, parts of an A haplotype). Of immunologic relevance, the “A” haplotype encodes inhibitory KIR for all known HLA ligands; and, at most, a single activating KIR expressed on the NK-cell surface, *KIR2DS4* being often represented by an aberrant allele (14). In contrast, “B” haplotypes are distinguished by one or more of the following features: they encode several activating KIR; lack one or more genes for the aforementioned inhibitory KIR; and/or carry *KIR2DL5*, of uncertain biological role (15). This diversity appears to influence many human health conditions (16).

Certain neighbor *KIR* genes tend to appear strongly linked in the same haplotype. Noteworthy among those is the pair formed by *KIR 2DL5* and either *2DS3* or *2DS5*, these being inherited like allotypes of the same locus (17). This *KIR 2DL5–2DS3/5* cluster duplicated and diversified jointly during human evolution, and is seen on either or both of the centromeric or the telomeric intervals of many B haplotypes (8, 15, 17, 18). Existence of two such long and highly similar stretches of sequence favored further asymmetric recombination between the paralogous regions. This resulted in expanded and shortened haplotypes bearing tandem duplications or deletions of the intervening genes, as shown by us and others (9, 10, 15, 19–24). Additional consequences

of asymmetric recombination are novel fusion genes encoding chimeric KIR that blend structural and functional features of their parent receptors.

Initial studies of human *KIR* genotypes faced this vast polymorphism without previous knowledge of the structure and forms of variation of the *KIR*-gene complex, revealing multiple *KIR*-gene and allele profiles in different individuals, which could give a false impression of randomness (11, 25). Order, in the form of knowledge on common and variant patterns of association between *KIR* genes and alleles, emerged from subsequent studies of population groups and families; and from phasing and physical mapping of partial and complete *KIR*-gene haplotypes by DNA sequencing (4, 6–10, 26–29). Those studies were complemented by others focused on estimation of CNV and allelic diversity (23, 24, 30–39). In parallel, *KIR*-gene profiles were studied in many healthy and diseased populations and ethnic groups worldwide (40). However, many those population studies have benefited surprisingly little from knowledge gained in the last years on the structure and patterns of variability of the *KIR* gene complex, and, for many human populations, only collections of *KIR*-gene profiles and superficial analyses of the basic variations are available. Here, we have applied current knowledge of *KIR*-gene arrangements to a comprehensive analysis of the gene profiles observed in a European Mediterranean population.

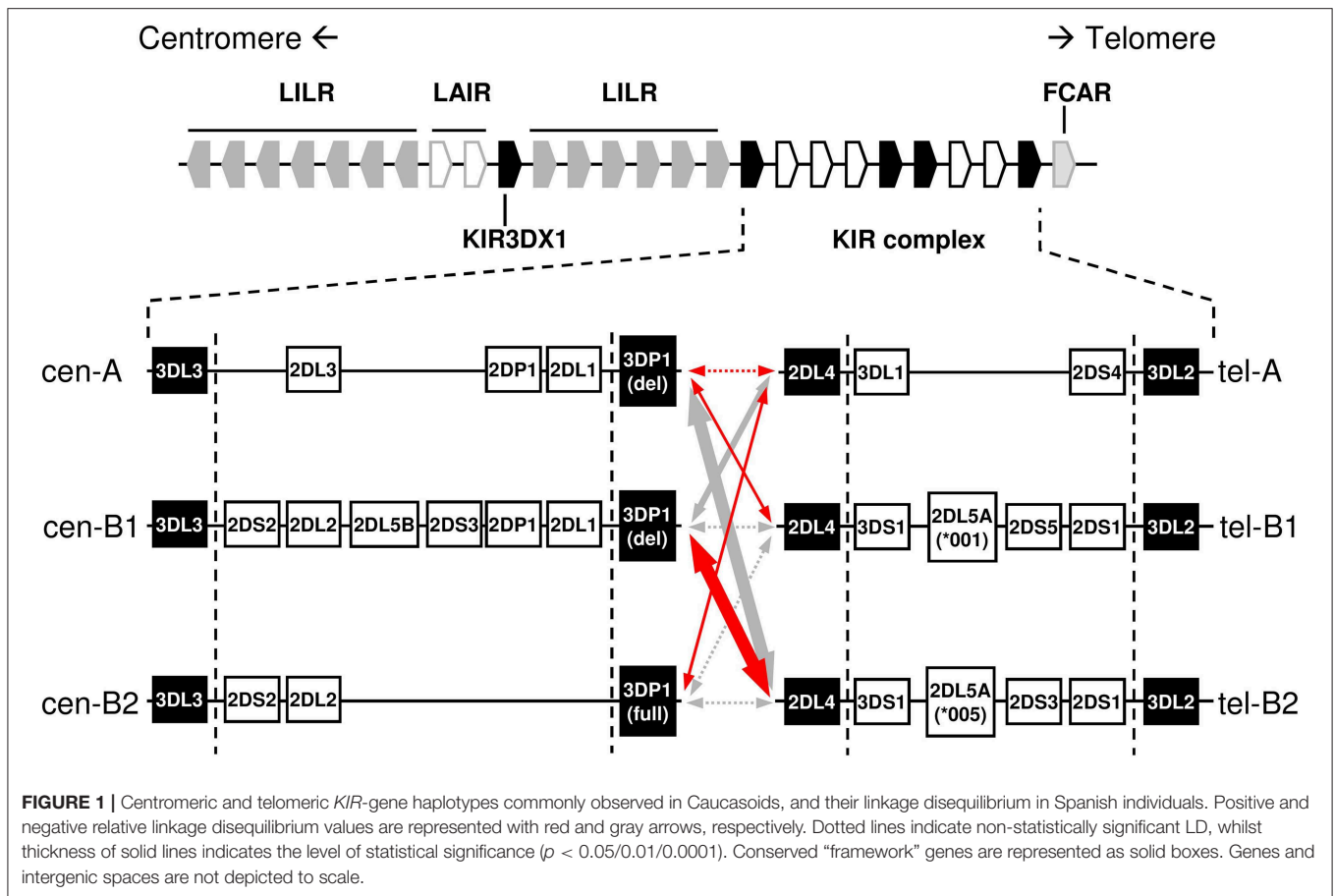
MATERIALS AND METHODS

Samples

Genomic DNA was isolated using standard methods from peripheral blood or mononuclear cell (PBMC) suspensions, obtained by Ficoll-Hypaque density gradient centrifugation (Lymphoprep, Axis-Shield PoC AS, Oslo, Norway), from 414 unrelated voluntary donors recruited in our centers in Madrid and Barcelona, mostly of Caucasoid origin; only known exceptions were two donors of mixed Hispanic/Amerindian ancestry, neither of whom contributed novel or variant gene profiles. Complementary DNA was synthesized with the AffinityScript Multiple Temperature cDNA Synthesis Kit (Agilent Technologies, Santa Clara, CA, USA) from 400 ng of total RNA, extracted from PBMCs of selected donors using the RNeasy Plus Mini kit (Qiagen GmbH, D-40724, Hilden, Germany).

KIR Genotyping

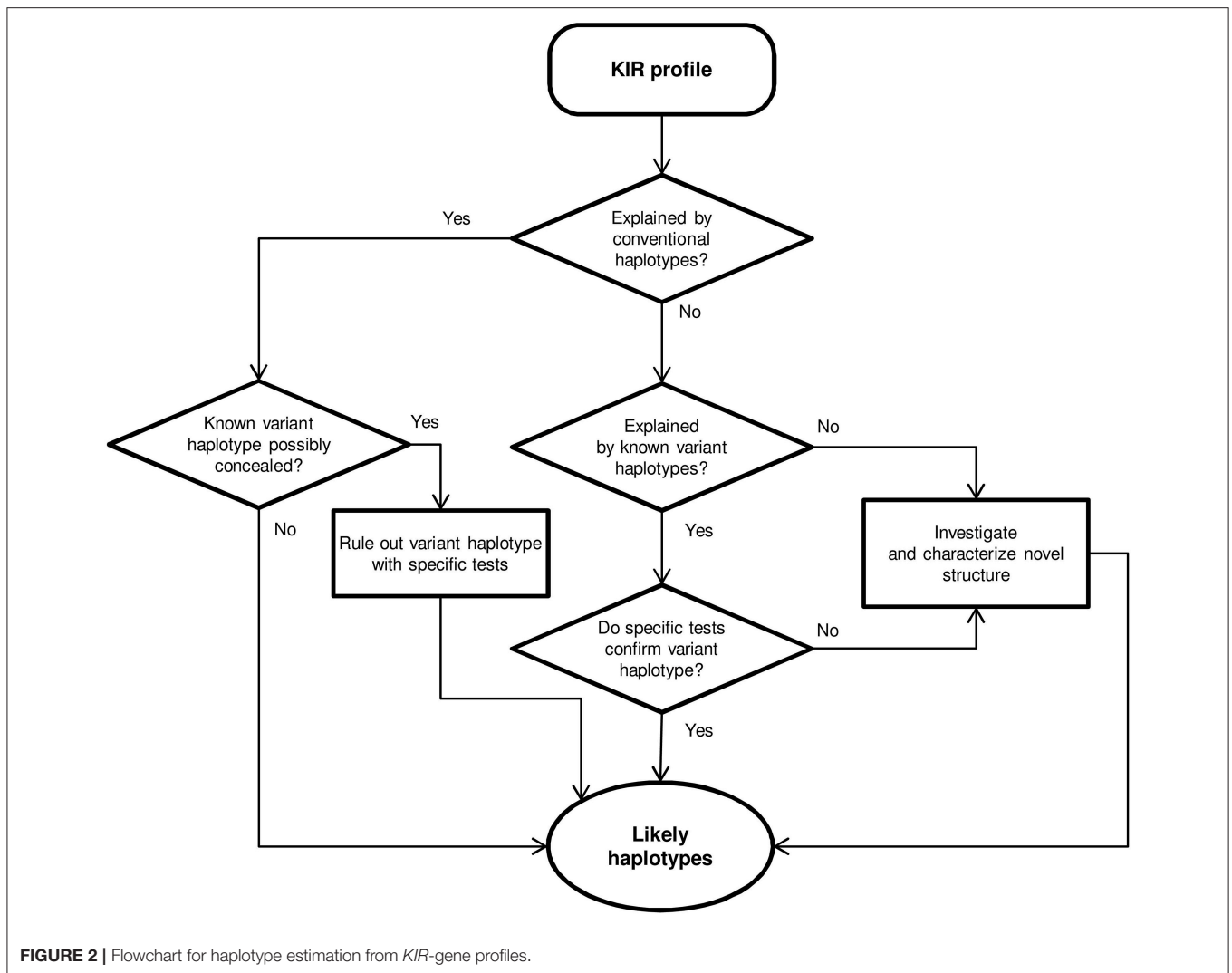
KIR genes, structural variants of *KIR 2DS4*, *2DL5*, and *3DP1*, and the hybrid alleles *2DS2*005* and *3DP1*004* were typed by PCR with sequence-specific primers (SSP), as previously described (22, 41–43). Non-standard *KIR*-gene profiles were confirmed utilizing a commercial reverse oligonucleotide probe-hybridization method based on the Luminex xMap Technology (LabType SSO Test, One Lambda Inc., Canoga Park, CA). To verify presence of an expanded haplotype in a *3DP1*004^{ve}* donor, existence of three *KIR3DL1/S1* alleles was verified by sequence-based typing of exons 3–5 in two overlapping amplicons. Each of these was generated with Advantage-2 polymerase (BD-Clontech, Palo Alto, CA, USA)



and primer mixes F153/Rt624 (5′-tggtcaggacaarccctt-3′, exon 3; 5′-aggtccctgcaaggca-3′, exon 4) or Fg539/Rc959 (5′-actctttctgcacaagagg-3′, exon 4; 5′-cmactcgtaggagagtg-3′, exon 5). PCR conditions were: 1 min at 95°C, then 10 cycles of 30 s at 94°C, 30 s at 64°C and 120 s at 72°C; 20 cycles of 30 s at 94°C, 30 s at 60°C and 120 s at 72°C; final elongation of 10 min at 72°C. Exon sequences were determined using internal primers (not shown). To assess presence of a *KIR3DL1/L2* chimera (*3DL1*060*) (44, 45), its third through fifth and seventh through ninth exons were amplified separately using, respectively, primer mixes Fi2c-201/Ri5+305 (5′-tctagtaagagtgcttctc-3′, intron 2; 5′-atgggctctgggaaatgga-3′, intron 5); and Fi6g-235/Ra1461 (5′-gagaaagcaggagaaagctg-3′, intron 6; 5′-gttcattggatctggcaacct-3′, exon 9). PCR conditions were: for exons 2–5, 2 min at 95°C; 5 cycles of 30 s at 94°C, 30 s at 60°C and 90 s at 72°C; 25 cycles of 30 s at 94°C, 30 s at 56°C and 90 s at 72°C; and 7 min at 72°C; and for exons 7–9, 2 min at 95°C, 5 cycles of 30 s at 94°C, 30 s at 66°C and 90 s at 72°C; 25 cycles of 30 s at 94°C, 30 s at 62°C and 90 s at 72°C; and 7 min at 72°C. Genotyping was submitted on a regular basis to the external proficiency tests organized by the UCLA Immunogenetics Center (International KIR DNA exchange) to ensure its sensitivity, specificity and consistency, by means of comparison with the results obtained by other labs on samples distributed by the provider.

Haplotype Assignment

Centromeric and telomeric *KIR*-gene arrangements were inferred in each individual by comparing their gene profile with the common and well-characterized haplotypes shown in **Figure 1**, assuming as few atypical or unknown combinations as possible. In particular, with the exceptions mentioned in the Results section, the following general assumptions were made, based on previous physical mapping and family segregation analyses, and on linkage disequilibrium (LD) between genes, confirmed in our samples using PHASE v2.1 software (46, 47) (results not shown): (i) *KIR 2DP1-2DL1*, and *3DL1-2DS4* are fixed blocks in complete linkage. (ii) Full and deleted *3DP1* variants mark cen-B2 and cen-A/cen-B1 haplotypes, respectively. (iii) Members of pairs *3DL1/3DS1*, and *2DL3/2DL2* behave as alleles of the same locus. (iv) Similarly, *2DS3* and *2DS5* were considered allotypes of a duplicated locus, associating invariably with *2DL5*. (v) The duplicated *2DL5-2DS3/S5* cluster was assigned to the centromeric or the telomeric sides, or both, according to presence or absence of adjacent genes: *2DS2-2DL2* and *2DP1-2DL1* (centromeric); and *3DS1* and *2DS1* (telomeric). (vi) Ambiguities derived from the latter rule were solved by *2DL5* subtyping and taking into account the fixed associations of *2DL5A*001* with *2DS5* and *2DL5A*005* with *2DS3* in tel-B1 and tel-B2 haplotypes, respectively (15, 41); besides those of *2DL5B* with *3DP1*003* and centromeric forms of *2DS3* (or, rarely in



Caucasoids, *2DS5*). As shown in **Figure 2**, and detailed in Results, *KIR* gene profiles not fitting with these rules were then compared with contracted and expanded haplotypes described in detail by us and others, and presence of these or new arrangements was verified, when appropriate, by genotyping characteristic traits, such as hybrid genes, or characterized by *de novo* sequencing. Complete haplotypes were assigned only when linkage in cis of centromeric and telomeric motifs was unambiguous; a common ambiguity was presence of two different motifs on both the centromeric and the telomeric intervals, circumstance in which no complete haplotypes were assigned. Relative linkage disequilibrium (D') between common centromeric and telomeric haplotypes, and its statistical significance were estimated with CubeX (48).

Characterization of *KIR2DL3*033*

A new *KIR2DS2/2DL3* hybrid was identified by sequencing a partial genomic fragment amplified with primers for exons 5 and 9 (details available upon request). To fully characterize the new

hybrid *KIR*, *2DL3*033*, we amplified its complete gene by long-range PCR, using Advantage-2 polymerase mix; forward primer LFc-444 (5'-gctattctgatgcctctggttagtac-3'), which recognizes a sequence conserved 5' of most *KIR*, but not in previously known *2DL3* alleles; and the reverse primer LRt1375 (5'-caggagacaactttggatca-3'), specific for a stop codon unique of *2DL3*. PCR conditions were: 2 min at 95°C; 5 cycles of 20 s at 94°C, 30 s at 68°C and 15 min at 72°C; 30 cycles of 20 s at 94°C, 30 s at 64°C; and 15 min at 72°C. The ~14-Kbp amplicon, spanning from the 5'UT region to the stop codon, was sequenced with internal primers. Confirmatory sequences for the *KIR2DL3*033* stop codon and its new polymorphisms in introns 6 and 7 were obtained from an additional 3.7-Kbp amplicon generated with forward primer Fi6t+1516, (5'-catcctaagtagctggataact-3', intron 6) and reverse primer Rt1460 (5'-acattggagctggcaacca-3', 3'UT), using the following PCR profile: 2 min at 95°C; 10 cycles of 20 s at 94°C, 30 s at 65°C and 4 min at 72°C; 20 cycles of 20 s at 94°C, 30 s at 61°C; and 4 min at 72°C.

To map *KIR2DL3*033* within the KIR complex, gene walking (26, 41) was carried out – a ~7-Kbp amplicon spanning exons 7–9 of the preceding gene, the intergenic region and exons 1–4 of the target gene was generated by PCR for 2 min at 95°C; 30 cycles of 20 s at 94°C and 15 min at 72°C; and 20 min at 72°C with a *KIR*-generic forward primer (Fi6–81, 5′-ctaaagagacgttgatgtgtgtacc–3′, intron 6) and the gene-specific reverse primer LRa546 (5′-ctccaatgaggtgcaaaagtctctat–3′, exon 4).

Presence of *KIR2DL3*033* in genomic DNA samples was screened by PCR-SSP, using BioTaq DNA polymerase (Biolone, London, UK) and primer mix Fi6t+1516/Ri6t+2713 (5′-catcctaaagtactgggataact–3′ and 5′-tctgtgctggaggattctga–3′), which recognizes a combination of polymorphisms unique to intron 6 of the *KIR2DS2/2DL3* hybrid, generating a 1387-bp amplicon. A primer pair recognizing a non-polymorphic sequence of the *COCH* gene served as an internal positive control of ~2 Kbp (*COCH*-Fi8–86, gaaagaactgtgtgtgtctggt; *COCH*-Ri11+95, atgggttaaagccacaggtgtttg). PCR conditions were: initial denaturation for 2 min at 95°C; 10 cycles of 20 s at 94°C, 30 s at 65°C and 90 s at 72°C; 20 cycles of 20 s at 94°C, 30 s at 61°C and 90 s at 72°C; and 7 min at 72°C.

Genomic Characterization of *KIR2DL5B*0020202*

The complete coding region and part of the intervening introns of the new allele *KIR2DL5B*0020202* were derived from a ~9.4-Kbp fragment generated from donor D139 by long range PCR with primer mix Fg–97b/Rg1769b (5′-tcaccctccrctgatgtg–3′, promoter region; and 5′-ggaaggtggaacagcagctgtctc–3′, 3′UTR) and Advantage-2 polymerase. PCR conditions were: 2 min at 95°C; 30 cycles of 20 s at 94°C and 15 min at 72°C; and 20 min at 72°C. The relative position of this allele in the *KIR* complex was determined by gene walking (26, 41). Identical procedures were used in another donor to identify and map *KIR2DL5B*0020106* (32).

DNA Sequencing and Nomenclature

PCR products were submitted, with no cloning step, to direct nucleotide sequencing in both strands, using internal primers (sequences available upon request). The products were analyzed in an ABI Prism 3100-Avant Genetic analyzer (Applied Biosystems) in the central DNA sequencing facility of *Instituto de Investigación Sanitaria Puerta de Hierro Segovia de Arana (IDIPHISA)*. The names *KIR2DL3*033* and *KIR2DL5B*0020202* (EMBL/GenBank/DDBJ database accession numbers HG931348 and LT604077, respectively) were officially assigned by the WHO Nomenclature Committee for factors of the HLA System, Subcommittee for Killer-cell Immunoglobulin-like Receptors (13).

Flow Cytometry

The NK-cell population was defined in PBMCs by the CD3⁺CD56⁺ phenotype, using anti-CD3-VioBlue (Miltenyi Biotec, Bergisch Gladbach, Germany) and anti-CD56-APC (eBioscience, Inc, San Diego, CA). These were combined in a donor carrying *KIR2DL3*033*, with anti-*KIR2DL3*-FITC

TABLE 1 | Carrier frequencies of *KIR* genes, pseudogenes, and their main structural and positional variants in 414 Spanish donors.

| Long tailed | | Short tailed | | Others | | | | |
|-------------|-------------|--------------|-------------|---------------|------|-------------|-----------------------|-------|
| Gene | Variant | % | Gene | Variant | % | Gene | Variant | % |
| <i>2DL1</i> | | 96.6 | <i>2DS1</i> | | 42.8 | <i>2DP1</i> | | 96.6 |
| <i>2DL2</i> | | 58.0 | <i>2DS2</i> | | 58.7 | <i>3DP1</i> | All | 100.0 |
| <i>2DL3</i> | | 88.4 | <i>2DS3</i> | All | 34.8 | | Exon 2 ⁺ | 31.4 |
| <i>2DL4</i> | | 100.0 | | Centromeric | 31.2 | | Exon 2 ^{del} | 96.6 |
| <i>2DL5</i> | All | 57.7 | | Telomeric | 15.2 | <i>3DX1</i> | | 100.0 |
| | Centromeric | 32.1 | <i>2DS4</i> | All | 95.9 | | | |
| | Telomeric | 41.5 | | Correct CDS | 36.2 | | | |
| <i>3DL1</i> | | 96.1 | | Frame-shifted | 82.1 | | | |
| <i>3DL2</i> | | 100.0 | <i>2DS5</i> | All | 30.0 | | | |
| <i>3DL3</i> | | 100.0 | | Centromeric | 0.0 | | | |
| | | | | Telomeric | 30.0 | | | |
| | | | <i>3DS1</i> | | 42.5 | | | |

CDS, coding sequence.

(180701, R&D Systems, Minneapolis, MN, USA) and anti-*KIR2DL3/L2/S2-PE/Cy7* (DX27, Miltenyi Biotec); and in donors bearing transcribed *KIR2DL5B*002* alleles, with anti-*KIR2DL5-PE* [UP-R1 (49), Biolegend, San Diego, CA, USA]. Isotype-matched negative controls were IgG1-PE (clone MOPC-21, Sigma-Aldrich, St. Louis, MO), IgG2a-FITC (clone MG2A01, Invitrogen, Camarillo, CA, USA), and IgG2a-PE (clone S43.10, Miltenyi Biotec). Flow cytometry analyses were performed in a MACSQuant Analyzer using MACSQuantify software (both by Miltenyi Biotec) in the central facility of *IDIPHISA*.

RESULTS

KIR-Gene Frequencies and Profiles

To characterize and understand the diversity of *KIR* genotypes in the Spanish population, we determined the *KIR*-gene content in the genome of 414 unrelated donors using a locally designed PCR-SSP (sequence-specific primers) method, which also discriminates between structural variants of *KIR 2DS4* and *3DP1*. Unusual genotypes were further investigated and confirmed using a combination of techniques, including, as appropriate, probe hybridization; selective sequencing of the relevant coding, non-coding or intergenic regions; and physical mapping of neighbor genes (*KIR*-gene “walking”), when relevant.

Individual *KIR*-gene frequencies are shown in **Table 1**. Framework *KIR* genes and pseudogenes *3DL3*, *3DP1*, *2DL4*, and *3DL2* were detected in every donor, even though seven of them were then deduced to lack *3DP1-2DL4-3DL1/S1*, or have *3DL2* partially deleted, on one chromosome. Also found in all 414 donors was *KIR3DX1*, a gene of uncertain function located outside and 180 Kbp centromeric to the *KIR* complex, which is seldom typed for. Of note, only the latter gene and *KIR3DL3*, both of unknown biological significance (5, 50), appear to be truly conserved (i.e., not submitted to CNV) among human *KIR*.

Non-framework genes encoding long-tailed KIR typical of A-haplotypes *2DL1*, *2DL3*, and *3DL1* had frequencies of ~90%; whilst *2DL2* and *2DL5*, encoding inhibitory KIR characteristic of B-haplotypes were seen in ca. 60% of the donors. Activating *KIR*-gene frequencies were more variable, ranging from 30.0% (*2DS5*) to 95.9% (*2DS4*). The latter was most often represented by frame-shifted alleles (82.1 vs. 36.2% alleles with canonical coding sequence), therefore the most common functional activating *KIR* was actually *2DS2* (58.7%) (**Table 1**).

Based on *KIR*-gene content, we found 38 different profiles, which were sorted into three groups: (i) the AA profile carrying exclusively genes of the A haplotype (24.15% of individuals); (ii) 16 BX profiles having all genes of the A-haplotype plus one or more B-haplotype genes (61.12%); and (iii), 21 BB profiles, defined by presence of B-haplotype genes and lack of one or more genes of the A-haplotype (14.73% of individuals). The individual and grouped frequencies of those profiles are shown in **Figures 3A,B**. The AA genotype was most frequent (ID: 1, 24.15%), followed by six BX genotypes (ID: 4, 2, 5, 7, 3 and 6) which, together, account for more than 50% of individuals; and by the two most common BB profiles (ID: 71 and 72; 3.14 and 2.66%, respectively). The overall distribution of *KIR*-gene frequencies and profiles observed in our sample is not dissimilar from those reported in other Caucasoid populations, and it is also consistent with those found in other large samples of Spanish individuals (40, 51–53).

A cumulative frequency analysis of the distribution of *KIR* genotypes is shown in **Figure 3C**. More than 50% of the population can be represented by three genotypes; six genotypes account for 75% of the total; and 13 are needed to explain 90% of the diversity. The remaining 10% is accounted for by 25 gene profiles, 14 of which were observed only once. As analyzed in more detail below, more than one third of the gene profiles (fourteen genotypes, belonging to 20 individuals) cannot be explained by any homo- or heterozygous combination of canonical haplotypes.

Centromeric and Telomeric Interval Analysis

Following a parsimonious approach that assumed as few non-canonical or novel *KIR*-gene arrangements as possible, we assigned each gene profile to the most likely diploid combination of well-known centromeric and telomeric haplotypes seen in most ethnicities (**Figure 1**). This was possible in 394 donors (95.17%), and the frequencies of their centromeric and telomeric deduced genotypes are represented in **Figure 4A**. On the centromeric region, the cen-AA genotype was most common (40.34%), followed by combinations of cen-A with either cen-B1 or cen-B2 haplotypes, seen with even frequencies—21.23 and 22.95%, respectively. Much less frequent were combinations of only cen-B1 or -B2 motifs, each seen at <5%. Centromeric motifs consistently associated with the major *KIR3DP1* allotypes (exon 2^{+/del}) as reported (54), with a single exception described previously by us [haplotype *2DS2-2DL2-3DP1^{del}* in family C180 (43)]. On the telomeric side, the combination of two tel-A segments was again most common

at 55.07%; followed by combinations of tel-A and tel-B motifs (24.88% tel-AB1 and 11.35% tel-AB2); whereas combinations of tel-B1 or -B2 haplotypes collectively represented only 3.83% of telomeric genotypes.

From the previous genotypes, and from those eventually assigned to individuals with unconventional profiles (following section), we estimated the frequencies of individual centromeric and telomeric haplotypes (**Figure 4B**). Also based on those assignments of partial centromeric and telomeric motifs, entire basic haplotypes (i.e., A vs. B) could be phased in 81% of donors (i.e., those who, on at least one of their telomeric or centromeric segments, only had either A or B profiles, but not both). This allowed a minimum estimate of the frequency of such complete basic haplotypes (**Figure 4C**): at least 45% of haplotypes are A (cen-A/tel-A), whilst more than 36% of haplotypes would be of the B-type (cen-A/tel-B, cen-B/tel-A, or cen-B/tel-B). The remaining ~19% of haplotypes could not be unambiguously assigned to the A- or the B-groups, because coincidence of A and B profiles on both the centromeric and the telomeric regions of the same individual precluded phasing.

Linkage disequilibrium between common centromeric and telomeric motifs is analyzed in **Table 2**, and depicted in **Figure 1**. Of note, association between cen-A and tel-A haplotypes was weak ($D' = 0.089$) and non-significant, suggesting that their common composition of a complete A haplotype is explained merely by the high frequency of its two segments. In contrast, strong were the positive LD of tel-B2 (*KIR 3DS1-2DL5-2DS3-2DS1*) with cen-B1, and its negative LD with cen-A (0.70 and -0.73, respectively; $p < 0.0001$). As previously noted (17), this means that the telomeric cluster *2DL5A*005-2DS3*002* is most often associated with a nearly identical sequence (*2DL5B*002-2DS3*001*) on the centromeric segment of the same haplotype, perhaps a reminiscence of their recent common origin.

Taken together, only 24 of the 38 observed *KIR*-gene profiles were explained by combinations of canonical centromeric and telomeric motifs; whilst no such combination could account for 14 profiles (i.e., more than one third), which owed to 2.66% of all chromosomes carrying atypical *KIR*-gene arrangements, as analyzed in the following sections.

KIR Gene Profiles Explained by Known Non-canonical Arrangements

Twenty individuals (4.8%) had *KIR* genotypes unexplained by any homo- or heterozygous combination of conventional haplotypes. Of those, 17 could be explained, as detailed below, by recombinant or variant structures previously described by us and others. Furthermore, specific tests targeting marker polymorphisms disclosed two additional donors in whom atypical haplotypes were concealed under apparently canonical *KIR* profiles, making a total of 22 individuals (5.3%) with unusual *KIR*-gene arrangements (**Figure 5**). Finally, three donors carried new haplotypes or hybrid genes characterized in the following sections.

Centromeric Interval

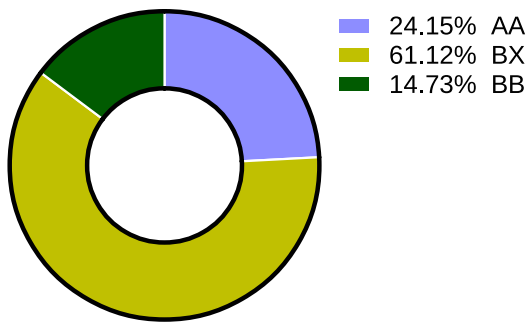
Two atypical profiles with singularities affecting only the centromeric region were found in seven donors. One of them

A

| Standard profiles | | | | | | | | | | | | | | | | | N = 414 | | | | |
|-------------------|-------|------|------|------|------|-------|------|------|------|------|----------|------|------|------|------|-------|---------|------|------|------|-------|
| ID | Group | 3DX1 | 3DL3 | 2DS2 | 2DL2 | 2DL5B | 2DS3 | 2DL3 | 2DP1 | 2DL1 | 3DP1 | 2DL4 | 3DL1 | 2DS4 | 3DS1 | 2DL5A | 2DS5 | 2DS3 | 2DS1 | 3DL2 | % |
| 1 | AA | 3DX1 | 3DL3 | | | | | 2DL3 | 2DP1 | 2DL1 | del | 2DL4 | 3DL1 | 2DS4 | | | | | | 3DL2 | 24,15 |
| 2 | BX | 3DX1 | 3DL3 | | | | | 2DL3 | 2DP1 | 2DL1 | del | 2DL4 | 3DL1 | 2DS4 | 3DS1 | 2DL5A | 2DS5 | | 2DS1 | 3DL2 | 13,77 |
| 8 | BX | 3DX1 | 3DL3 | | | | | 2DL3 | 2DP1 | 2DL1 | del | 2DL4 | 3DL1 | 2DS4 | 3DS1 | 2DL5A | | 2DS3 | 2DS1 | 3DL2 | 1,21 |
| 69 | BB | 3DX1 | 3DL3 | | | | | 2DL3 | 2DP1 | 2DL1 | del | 2DL4 | | | 3DS1 | 2DL5A | 2DS5 | | 2DS1 | 3DL2 | 1,21 |
| 5 | BX | 3DX1 | 3DL3 | 2DS2 | 2DL2 | 2DL5B | 2DS3 | 2DL3 | 2DP1 | 2DL1 | del | 2DL4 | 3DL1 | 2DS4 | | | | | | 3DL2 | 9,42 |
| 6 | BX | 3DX1 | 3DL3 | 2DS2 | 2DL2 | 2DL5B | 2DS3 | 2DL3 | 2DP1 | 2DL1 | del | 2DL4 | 3DL1 | 2DS4 | 3DS1 | 2DL5A | 2DS5 | | 2DS1 | 3DL2 | 3,87 |
| 7 | BX | 3DX1 | 3DL3 | 2DS2 | 2DL2 | 2DL5B | 2DS3 | 2DL3 | 2DP1 | 2DL1 | del | 2DL4 | 3DL1 | 2DS4 | 3DS1 | 2DL5A | | 2DS3 | 2DS1 | 3DL2 | 6,76 |
| 70 | BB | 3DX1 | 3DL3 | 2DS2 | 2DL2 | 2DL5B | 2DS3 | 2DL3 | 2DP1 | 2DL1 | del | 2DL4 | | | 3DS1 | 2DL5A | 2DS5 | | 2DS1 | 3DL2 | 0,24 |
| 70 | BB | 3DX1 | 3DL3 | 2DS2 | 2DL2 | 2DL5B | 2DS3 | 2DL3 | 2DP1 | 2DL1 | del | 2DL4 | | | 3DS1 | 2DL5A | 2DS5 | 2DS3 | 2DS1 | 3DL2 | 0,94 |
| 4 | BX | 3DX1 | 3DL3 | 2DS2 | 2DL2 | | | 2DL3 | 2DP1 | 2DL1 | full/del | 2DL4 | 3DL1 | 2DS4 | | | | | | 3DL2 | 14,98 |
| 3 | BX | 3DX1 | 3DL3 | 2DS2 | 2DL2 | | | 2DL3 | 2DP1 | 2DL1 | full/del | 2DL4 | 3DL1 | 2DS4 | 3DS1 | 2DL5A | 2DS5 | | 2DS1 | 3DL2 | 6,28 |
| 7 | BX | 3DX1 | 3DL3 | 2DS2 | 2DL2 | | | 2DL3 | 2DP1 | 2DL1 | full/del | 2DL4 | 3DL1 | 2DS4 | 3DS1 | 2DL5A | | 2DS3 | 2DS1 | 3DL2 | 1,21 |
| 70 | BB | 3DX1 | 3DL3 | 2DS2 | 2DL2 | | | 2DL3 | 2DP1 | 2DL1 | full/del | 2DL4 | | | 3DS1 | 2DL5A | 2DS5 | 2DS3 | 2DS1 | 3DL2 | 0,24 |
| 159 | BB | 3DX1 | 3DL3 | 2DS2 | 2DL2 | | | 2DL3 | 2DP1 | 2DL1 | full/del | 2DL4 | | | 3DS1 | 2DL5A | | 2DS3 | 2DS1 | 3DL2 | 0,24 |
| 71 | BB | 3DX1 | 3DL3 | 2DS2 | 2DL2 | 2DL5B | 2DS3 | | 2DP1 | 2DL1 | del | 2DL4 | 3DL1 | 2DS4 | | | | | | 3DL2 | 0,72 |
| 73 | BB | 3DX1 | 3DL3 | 2DS2 | 2DL2 | 2DL5B | 2DS3 | | 2DP1 | 2DL1 | del | 2DL4 | 3DL1 | 2DS4 | 3DS1 | 2DL5A | 2DS5 | | 2DS1 | 3DL2 | 0,24 |
| 90 | BB | 3DX1 | 3DL3 | 2DS2 | 2DL2 | 2DL5B | 2DS3 | | 2DP1 | 2DL1 | del | 2DL4 | 3DL1 | 2DS4 | 3DS1 | 2DL5A | | 2DS3 | 2DS1 | 3DL2 | 1,45 |
| 81 | BB | 3DX1 | 3DL3 | 2DS2 | 2DL2 | 2DL5B | 2DS3 | | 2DP1 | 2DL1 | del | 2DL4 | | | 3DS1 | 2DL5A | 2DS5 | 2DS3 | 2DS1 | 3DL2 | 0,72 |
| 190 | BB | 3DX1 | 3DL3 | 2DS2 | 2DL2 | 2DL5B | 2DS3 | | 2DP1 | 2DL1 | del | 2DL4 | | | 3DS1 | 2DL5A | | 2DS3 | 2DS1 | 3DL2 | 0,24 |
| 71 | BB | 3DX1 | 3DL3 | 2DS2 | 2DL2 | 2DL5B | 2DS3 | | 2DP1 | 2DL1 | full/del | 2DL4 | 3DL1 | 2DS4 | | | | | | 3DL2 | 3,14 |
| 73 | BB | 3DX1 | 3DL3 | 2DS2 | 2DL2 | 2DL5B | 2DS3 | | 2DP1 | 2DL1 | full/del | 2DL4 | 3DL1 | 2DS4 | 3DS1 | 2DL5A | 2DS5 | | 2DS1 | 3DL2 | 0,24 |
| 90 | BB | 3DX1 | 3DL3 | 2DS2 | 2DL2 | 2DL5B | 2DS3 | | 2DP1 | 2DL1 | full/del | 2DL4 | 3DL1 | 2DS4 | 3DS1 | 2DL5A | | 2DS3 | 2DS1 | 3DL2 | 0,72 |
| 72 | BB | 3DX1 | 3DL3 | 2DS2 | 2DL2 | | | | | | full | 2DL4 | 3DL1 | 2DS4 | | | | | | 3DL2 | 2,66 |
| 76 | BB | 3DX1 | 3DL3 | 2DS2 | 2DL2 | | | | | | full | 2DL4 | 3DL1 | 2DS4 | 3DS1 | 2DL5A | 2DS5 | | 2DS1 | 3DL2 | 0,48 |
| Variant profiles | | | | | | | | | | | | | | | | | | | | | |
| 58 | BX | 3DX1 | 3DL3 | | 2DL2 | 2DL5B | 2DS3 | 2DL3 | 2DP1 | 2DL1 | del | 2DL4 | 3DL1 | 2DS4 | 3DS1 | 2DL5A | 2DS5 | | 2DS1 | 3DL2 | 0,24 |
| 10 | BX | 3DX1 | 3DL3 | 2DS2 | | | | 2DL3 | 2DP1 | 2DL1 | del | 2DL4 | 3DL1 | 2DS4 | | | | | | 3DL2 | 0,48 |
| 12 | BX | 3DX1 | 3DL3 | 2DS2 | | | | 2DL3 | 2DP1 | 2DL1 | del | 2DL4 | 3DL1 | 2DS4 | 3DS1 | 2DL5A | 2DS5 | | 2DS1 | 3DL2 | 0,48 |
| 118 | BB | 3DX1 | 3DL3 | 2DS2 | 2DL2 | | | | 2DP1 | 2DL1 | del | 2DL4 | 3DL1 | 2DS4 | 3DS1 | 2DL5A | 2DS5 | | 2DS1 | 3DL2 | 0,24 |
| 30 | BX | 3DX1 | 3DL3 | | | 2DL5B | 2DS3 | 2DL3 | 2DP1 | 2DL1 | del | 2DL4 | 3DL1 | 2DS4 | | | | | | 3DL2 | 0,48 |
| 9 | BX | 3DX1 | 3DL3 | 2DS2 | 2DL2 | 2DL5B | | 2DL3 | 2DP1 | 2DL1 | del | 2DL4 | 3DL1 | 2DS4 | | | 2DS5 | | 2DS1 | 3DL2 | 0,48 |
| 11 | BX | 3DX1 | 3DL3 | 2DS2 | 2DL2 | 2DL5B | | 2DL3 | 2DP1 | 2DL1 | del | 2DL4 | 3DL1 | 2DS4 | | | | 2DS3 | 2DS1 | 3DL2 | 0,24 |
| 97 | BB | 3DX1 | 3DL3 | 2DS2 | 2DL2 | 2DL5B | | | | | full | 2DL4 | 3DL1 | 2DS4 | | | | 2DS3 | 2DS1 | 3DL2 | 0,24 |
| 91 | BB | 3DX1 | 3DL3 | 2DS2 | 2DL2 | 2DL5B | 2DS3 | | 2DP1 | 2DL1 | del | 2DL4 | 3DL1 | 2DS4 | | | 2DS5 | | 2DS1 | 3DL2 | 0,24 |
| 113 | BB | 3DX1 | 3DL3 | 2DS2 | 2DL2 | 2DL5B | 2DS3 | | 2DP1 | 2DL1 | del | 2DL4 | 3DL1 | 2DS4 | | | | 2DS3 | 2DS1 | 3DL2 | 0,24 |
| 13 | BX | 3DX1 | 3DL3 | 2DS2 | 2DL2 | 2DL5B | 2DS3 | 2DL3 | 2DP1 | 2DL1 | full/del | 2DL4 | 3DL1 | 2DS4 | 3DS1 | | | | | 3DL2 | 0,72 |
| 94 | BB | 3DX1 | 3DL3 | 2DS2 | 2DL2 | 2DL5B | 2DS3 | | 2DP1 | 2DL1 | full/del | 2DL4 | 3DL1 | 2DS4 | 3DS1 | | | | | 3DL2 | 0,24 |
| 13 | BX | 3DX1 | 3DL3 | 2DS2 | 2DL2 | 2DL5B | 2DS3 | 2DL3 | 2DP1 | 2DL1 | del | 2DL4 | 3DL1 | 2DS4 | 3DS1 | 2DL5A | | | | 3DL2 | 0,24 |
| 331 | BX | 3DX1 | 3DL3 | | | | | 2DL3 | 2DP1 | 2DL1 | del | 2DL4 | 3DL1 | | 3DS1 | 2DL5A | 2DS5 | | 2DS1 | 3DL2 | 0,24 |

B

Basic genotypes



C

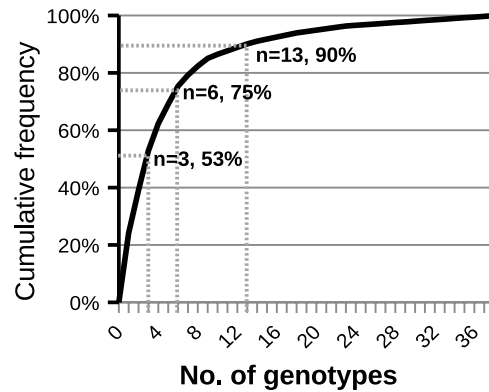


FIGURE 3 | *KIR*-gene profiles observed in a sample of Spanish individuals. **(A)** Gene presence or absence is represented by solid gray and empty boxes; allelic forms are indicated for *KIR3DP1*. Carrier frequency is given on the right side of each genotype. Gene order reflects, approximately, that seen in the *KIR* complex, with genes forming A-haplotypes in the middle, flanked on both sides by genes characteristic of B-haplotypes. For *KIR 2DL5* and *2DS3*, genes represented by two paralogues, a diagonal line indicates that the gene is present in a genotype, but most likely in the alternative location. The ID column shows the number by which the genotype is registered in www.allelefrequencies.net (40); since this database does not distinguish between structural/positional variants, a same ID can correspond to several profiles in the table. Two profiles (7 and 81) include each one individual bearing a concealed variant haplotype, as explained in the text. In the lower part of the panel, which compiles gene profiles not explained by conventional haplotypes, thick lines highlight distinctive traits, including missing genes normally associated with ones present in a given genotype. **(B)** Distribution of the major groups of *KIR* genotypes. **(C)** Cumulative frequencies of *KIR* profiles.

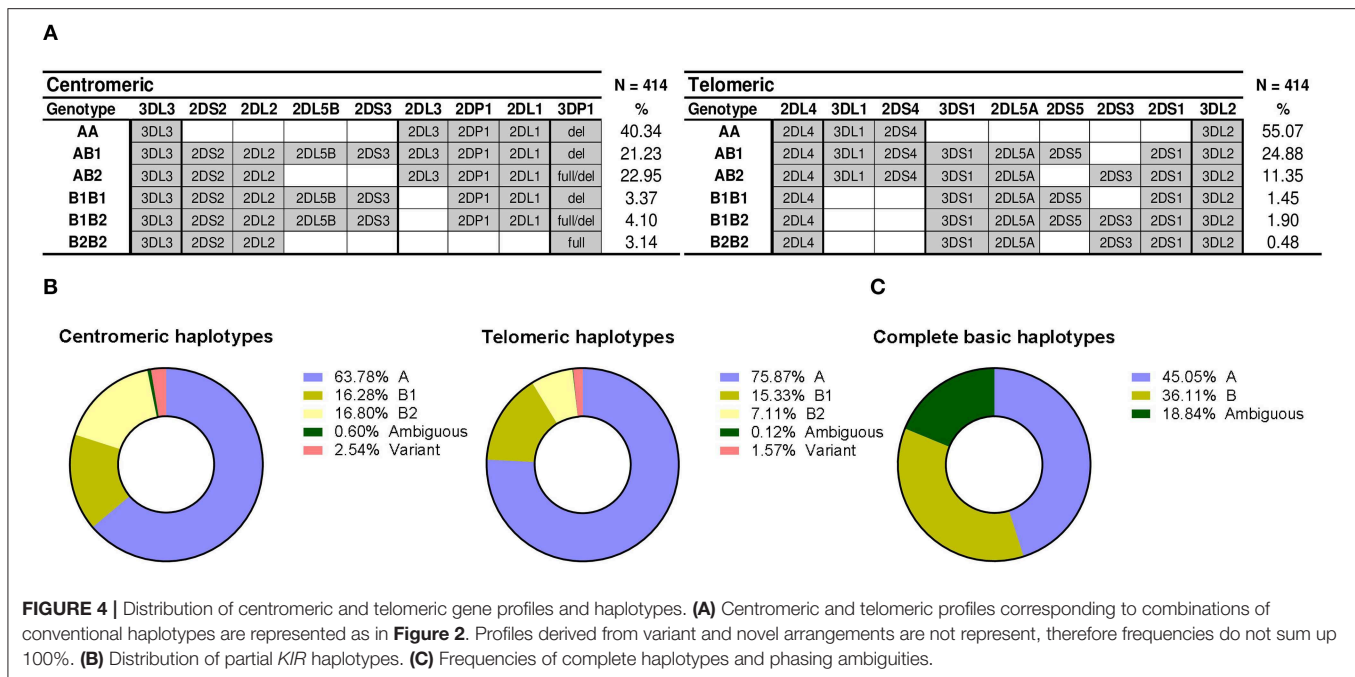


TABLE 2 | Linkage disequilibrium between centromeric and telomeric *KIR* haplotypes.

| hap. freq. | tel-A | tel-B1 | tel-B2 |
|------------|---------------|--------------|---------------|
| cen-A | 0.503 | 0.129 | 0.012 |
| | 0.089 | 0.546 | -0.727 |
| | n.s. | <0.05 | <-0.0001 |
| cen-B1 | 0.096 | 0.012 | 0.054 |
| | -0.253 | -0.534 | 0.702 |
| | <0.01 | n.s. | <-0.0001 |
| cen-B2 | 0.155 | 0.011 | 0.003 |
| | 0.692 | -0.574 | -0.775 |
| | <0.05 | n.s. | n.s. |

N.s., non-significant. Bold, statistically significant *D'* values.

presented *KIR2DL2* in absence of *2DS2*. This profile, initially characterized in Black individuals (8, 19), might be explained by *KIR2DS2* deletion from the usual *2DS2-2DL2* cluster; alternatively, since these two highly homologous genes possibly derive from a common ancestor, the variant profile might be reminiscent of the ancestral haplotype existing before the gene duplication that gave origin to the two paralogues (**Figure 5**).

Another five individuals had the reciprocal combination, i.e., *KIR2DS2* in isolation from *2DL2* and/or other cen-B1 characteristic genes, a profile typically seen in a shortened haplotype previously characterized by our group (43). Such haplotype, generated by unequal crossing-over between *KIR2DS2* and *2DS3*, is marked by the resulting chimeric allele, *KIR2DS2*005*, and by deletion of the intervening genes

(*KIR2DL2*, *2DL5B*, and *2DS3*). A PCR-SSP test specific for *KIR2DS2*005* confirmed this marker in three of the five suspected individuals; and disclosed it in another donor with an apparently standard *KIR* profile, in which lack of *KIR2DL2* within the recombinant haplotype was concealed by its presence on the other one.

The remaining two *KIR2DS2*⁺*-2DL2*⁻ individuals did not carry this shortened B haplotype, since they were negative in the *KIR2DS2*005* test. Instead, they carried a new recombinant haplotype and a novel hybrid gene, as analyzed in a separate section. Also described separately is the last variant centromeric profile, in which the *KIR 2DL5B-2DS3* cluster is seen in absence of its usual companions *2DS2-2DL2*.

Central Cluster

Affecting both the centromeric and the telomeric regions were haplotype arrangements that included duplications or deletions of the central framework genes, identified in 13 donors. For instance, an atypical profile marked by presence of *KIR 2DS3/2DS5* and *2DS1* in absence of *3DS1* was explained by previously characterized haplotypes bearing an extensive deletion affecting seven genes on the central region of the *KIR*-gene complex, including, among others, the otherwise conserved *KIR 3DP1*, *2DL4*, and *3DL1/3DS1* loci (19, 20). The resulting contracted B haplotype, containing only seven genes, generates an unusual juxtaposition of the centromeric *KIR2DL5B* and the telomeric *KIR2DS3/2DS5* loci. This profile was observed in six individuals, but in contrast with studies on other ethnic groups, the deletion of the central genes was never observed in homozygosis in this population sample. However, such genotype does exist among Spanish Caucasoids, as we reported earlier [donor LH304 (49)].

| Known variant haplotypes | Distinctive features | Freq. (n) |
|---------------------------|---|-----------|
| | <p>2DL2 in absence of 2DS2</p> <p>Associated profile: 58</p> | 0.24% (1) |
| | <p>2DS2/2DS3 hybrid (2DS2*005) in absence of 2DL2</p> <p>2DL2-2DL5B and partial 2DS2, 2DS3 deletions</p> <p>Associated profiles: 12, 118, 81 (concealed)</p> | 0.97% (4) |
| | <p>Deletion of 7 central genes in a B haplotype; often, 2DS1 in absence of 3DS1</p> <p>Associated profiles: 9, 11, 91, 97, 113</p> | 1.45% (6) |
| | <p>2DL5A/3DP1 hybrid (3DP1*004)</p> <p>Duplication of 3 central genes (3DP1, 2DL4, 3DL1/S1); often, 3DS1 in absence of 2DS1</p> <p>Associated profiles: 13, 94, 7 (concealed)</p> | 0.97% (5) |
| | <p>Duplication/insertion of 6 central genes</p> <p>Associated profile: 13</p> | 0.24% (1) |
| | <p>3DL1/3DL2 hybrid (3DL1*060)</p> <p>2DS4, and partial 3DL1, 3DL2 deletions</p> <p>Associated profile: 331</p> | 0.24% (1) |
| Newly observed haplotypes | Distinctive features | Freq. (n) |
| | <p>2DS2/2DL3 hybrid (2DL3*033) in absence of 2DL2</p> <p>Associated profile: 10</p> | 0.48% (2) |
| | <p>2DL5B-2DS3 cluster downstream of 2DL3</p> <p>Transcribed (Runx*) 2DL5B*002 alleles</p> <p>Associated profile: 30</p> | 0.48% (2) |

FIGURE 5 | Variant and novel haplotypes detected in Spanish individuals. Colors are used to highlight gene deletions and hybrid structures derived from recombination of two different genes or haplotypes, but they lack a specific meaning. Duplicated genes are represented in parallel.

Five individuals showed the opposite combination—*KIR3DS1* in absence of *2DS1* (and the telomeric *2DL5-2DS5/S3* group). This trait is typically seen associated with a tandem duplication of the *3DP1-2DL4-3DL1/S1* cluster and the recombinant, transcribed *KIR3DP1*004* allotype, a marker of this duplication (21, 22). This “full” (exon 2^{+ve}) *3DP1* allotype is often discordant at first glance with the centromeric profile, serving as a beacon of the expanded haplotype. Its presence in four of the five suspected individuals, as well as in one with an apparently normal genotype, was confirmed by specific PCR-SSP detection of the hybrid gene *KIR3DP1*004*.

A sixth donor with a similar *KIR* genotype (*3DS1^{+ve}-2DL5^{+ve}-2DS3^{+ve}-2DS1^{-ve}*) was, in contrast, negative for *3DP1*004*. Its atypical gene profile could instead be explained by presence of an expanded haplotype we described in one Irish Caucasoid (17). Such haplotype is characterized by an even larger duplication/insertion of six central *KIR* genes, due to unequal crossing-over between the intergenic regions of the telomeric and the centromeric *2DL5-2DS3* clusters (Figure 5). Consistently with such duplication, the donor had two *3DL1* alleles besides *3DS1* (not shown).

Telomeric Interval

Least common were variants affecting exclusively the telomeric *KIR* region—we observed a single unusual *3DL1^{+ve}-2DS4^{-ve}* profile, represented in one donor. In this individual, we identified another previously described hybrid gene, *KIR3DL1*060*, arising from an asymmetric recombination event that fused *3DL1* exons 1–5 with *3DL2* exons 6–9 (44, 45). Concomitant deletion of the intervening gene *KIR2DS4* explains this gene profile.

A Novel *KIR2DS2/KIR2DL3* Fusion Gene Within a Recombinant B/A Motif Challenges Conventional Gene and Haplotype Classification

One donor apparently presented *KIR2DS2* in isolation from other B-haplotype genes (i.e., in the context of an AA genotype), but, as stated earlier, was negative for *2DS2*005*, which marks the only known gene arrangement that could account for such profile (43). To characterize the putative *2DS2* gene in the novel gene profile, we amplified its exons 5 through 7 (encoding the D2 Ig-like domain, stem and transmembrane region) in a 7.6-Kbp genomic fragment. Analysis of this amplicon revealed, instead of a proper *KIR2DS2* gene, a new hybrid sequence, of which the 5′- and the 3′-ends were homologous to *2DS2* and *2DL3*, respectively. Based on this information, the new gene was then amplified in a single ~14-Kbp genomic fragment comprising all its exons and introns, and sequence analysis confirmed its hybrid nature—its 5′ side (down to nucleotide 2,075 of intron 6, ca. 11 Kbp) was identical to *2DS2*0010102*; whilst the rest of the gene (~3 Kbp through the stop codon) matched *2DL3*0020101*, except for three base substitutions: two unique in intron 6 (11586 A>G and 11849 C>T), and one in intron 7, shared with *2DL3*010* (13627 G>A). The hybrid sequence is likely the result of asymmetric (non-allelic)

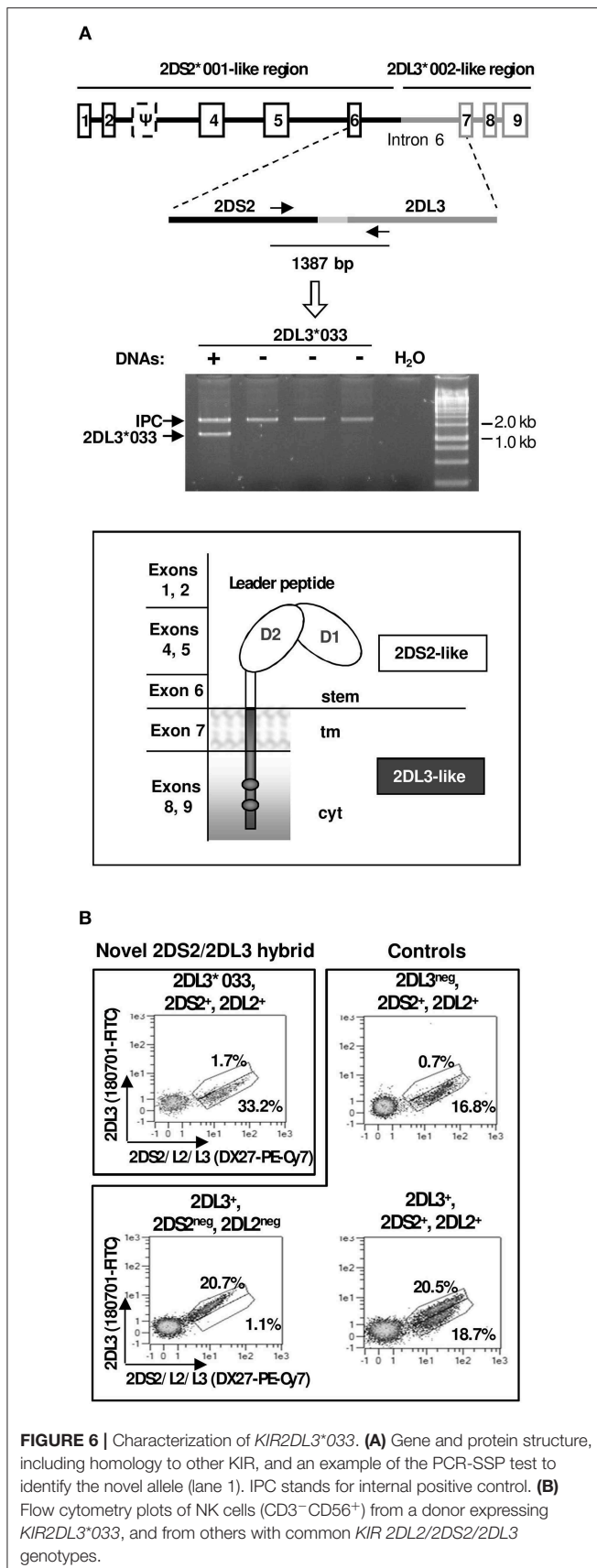
homologous recombination between *KIR2DS2* and *KIR2DL3* genes present in different B and A haplotypes, respectively. The apparent recombination spot is few bases upstream of an AluSX element (not shown).

As discussed later, the novel structure challenged unwritten rules followed previously to designate chimeric *KIR*, not sitting comfortably within any of the current designations. It was officially assigned to the *KIR2DL3* locus with the name *2DL3*033* by the *KIR* Nomenclature Committee, which reflects appropriately the fact that the encoded protein should have an intracellular inhibitory tail identical to those of most other *2DL3* alleles.

To map the new hybrid gene, we used a *KIR*-gene walking approach (i.e., amplification and sequencing of a genomic fragment spanning part of the gene of interest, and one in its vicinity), which showed *2DL3*033* to be located 3′ of *3DL3*, like common alleles of both its homologs *2DS2* and *2DL3* in conventional *KIR* haplotypes. Furthermore, the donor had *3DL3*003*, allele commonly linked to *2DS2* (24), in consonance with presence of a *2DS2*-like 5′ region in *2DL3*033*.

PBMCs of the donors in whom *KIR2DL3*033* was originally found were, unfortunately, unavailable. To estimate the *KIR2DL3*033* distribution and enable expression studies on this allele, we designed a PCR-SSP method targeting a specific combination of polymorphisms in its sixth intron, which led us to identify two additional examples of this allele in 1,101 DNA samples (~0.2%; confidence interval with $p < 0.05$: 0.00–0.46%). Using PBMC of one of those donors, we could readily amplify the *KIR2DL3*033* complete coding region (~1.1kb) by RT-PCR, demonstrating the normal transcription and processing of its mRNA. According to this, *KIR2DL3*033* encodes ligand-recognition Ig-like domains, and a stem homologous to those of the activating *2DS2*, but transmembrane and long intracytoplasmic regions like those of *2DL3* (Figure 6A). Therefore, the encoded receptor should combine the weak HLA-C1 recognition of the former, and the inhibitory capacity of the latter.

Since PBMCs of *KIR2DL3*033* donors with cenAA profiles were unavailable, we performed multicolour flow cytometry analyses of PBMCs of one available individual encoding *KIR2DL3*033* on one haplotype and the *2DS2-2DL2* combination on the second one. The observed lack of staining with a *KIR2DL3*-specific mAb (Figure 6B) was consistent with the *2DS2*-like nature of the *KIR2DL3*033* ectodomain. Unfortunately, the donor genotype precluded positive identification of cells expressing *KIR2DL3*033*, since these are indistinguishable with the available mAbs from those bearing its homologues *2DS2* and *2DL2*. Flow cytometry studies of further donors with favorable (i.e., cenAA) *KIR* profiles are warranted to demonstrate positively *KIR2DL3*033* NK-cell surface expression; this would be marked by presence of cells staining with DX27 (or equivalent mAbs), but not with reagents monospecific for conventional *KIR2DL3* alleles.



*KIR2DL5B*0020202*—A Transcribed Allele Linked to *KIR2DL3* in an Unusual Centromeric B Motif

Two individuals exhibited unusual presence of the *KIR 2DL5-2DS3* genes in absence of any other genes characteristic of *B* haplotypes, to which they are normally linked (i.e., *2DL2* or *3DS1*). To understand the unusual genotype, we used *KIR*-gene walking—amplification of a ~4-Kbp region spanning *KIR2DL5* exons 1–3, the last (ninth) exon of the unknown preceding gene, and the intergenic region. This enabled us to map, in both donors, *KIR2DL5B*002*-related sequences downstream of *KIR2DL3*010*. This arrangement is seemingly identical to one previously described in a minority of Black Africans (8, 9, 32, 55), in whom a *2DL5-2DS3* block is inserted between *2DL3* and *2DP1-2DL1* (Figure 5), thus converting a centromeric A-motif into a B-haplotype, according to the agreed definition of these.

To further characterize *KIR2DL5B* in the unusual haplotype, we amplified the whole gene by long-range PCR (~9 Kbp). Sequence analysis of this amplicon, along with that derived from *KIR*-gene walking, revealed, in one donor, a new *KIR2DL5B* allele, designated *KIR2DL5B*0020202*, in which a coding region identical to that of the previously known *KIR2DL5B*0020201* is fused to a “*KIR2DL5*-type III” promoter (15), similar to that found in the expressed allele *KIR2DL5B*003* (Figure 7A). This type of promoter retains an intact RUNX-binding site seen in all clonally expressed *KIR*, in contrast with common *KIR2DL5B* alleles, in which the site is destroyed by substitution of adenosine for guanosine –97, polymorphism completely associated with epigenetic silencing (41). Similar results were obtained in the second donor, in whom we found allele *KIR2DL5B*0020106*. This allele and the novel *KIR2DL5B*0020202* share a nearly identical combination of promoter and coding sequences, the latter differing by a single synonymous substitution (Figure 7B).

Conservation of the RUNX site in *KIR2DL5B*0020106* and **0020202* should, according to our hypothesis (41), confer these alleles a capacity to be transcribed, in contrast with most *2DL5B* alleles. To test this prediction, we performed RT-PCR experiments on RNA isolated from PBMC of donors D139 and 140016. Specific, correctly spliced amplicons were readily obtained for both *KIR2DL5B*0020106* and *KIR2DL5B*0020202* (Figure 7B), as verified by direct sequencing. This positive result opened the possibility of *KIR2DL5B* being expressed on the cell surface, which has never been shown. To explore this, we undertook flow-cytometry assays with the *KIR2DL5*-specific mAb UP-R1, but these showed no specific surface staining of peripheral blood NK cells (Figure 7C). This result is in line with the described behavior of allele *KIR2DL5A*005*, which shares with *KIR2DL5B*002* the identical sequence in the mature protein. Such protein, seemingly due to substitution of Ser for Gly174, is retained intracellularly in NK cells, besides reacting weakly with mAb UP-R1 (56); unfortunately, monoclonal antibodies for intracellular *KIR2DL5A*005/B*002* staining are unavailable.

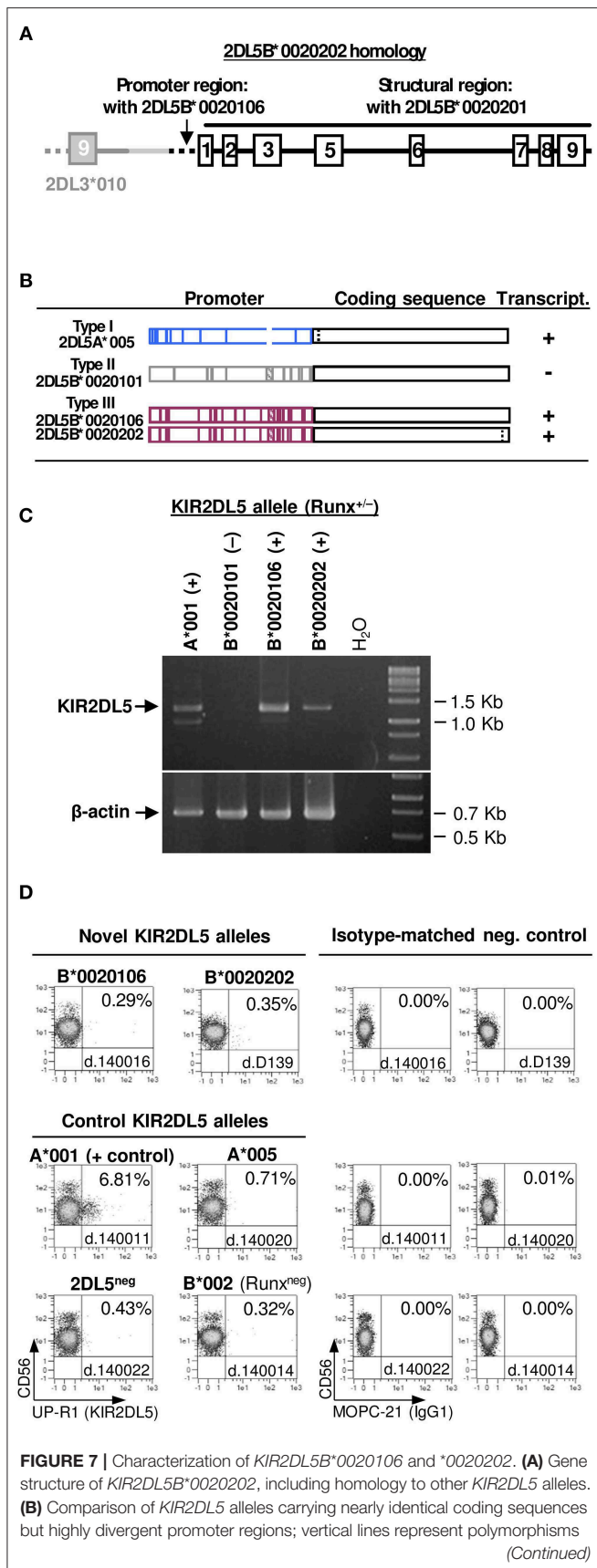


FIGURE 7 | distinguishing those alleles. Gene transcription or silencing is indicated on the right side. **(C)** RT-PCR assay showing *KIR2DL5B*0020106* and **0020202* transcription, in contrast with their common, silent homologue *KIR2DL5B*0020101*. Presence or absence of an intact RUNX binding site in the proximal promoter is indicated for each allele. **(D)** A *KIR2DL5* product is undetectable on the surface of NK cells transcribing *KIR2DL5B*0020106* and **0020202*, as we reported previously for *KIR2DL5A*005*, which encodes an identical mature polypeptide.

DISCUSSION

In-depth genomic studies have established the variable organization of the human *KIR* complex, defining gene motifs and extended haplotypes fixed in our species, and a series of variations from those, mostly generated by asymmetric (non-allelic) homologous recombination (4, 6–10, 26, 28, 29). In addition, sequence analyses based on Sanger and, more recently, second generation methods, have revealed the diversity of alleles commonly found in each of those *KIR* haplotypes (23, 24, 30–32, 34–39).

In parallel, the *KIR*-gene profiles of multiple populations worldwide have been explored in the last two decades, revealing that, whilst many *KIR* haplotypes and alleles are shared by humans of all ethnicities, notorious differences in their distribution exist, unveiling the evolutionary connections between human groups, and the variable selective pressures exerted on them by the environment (16, 40). However, it is noteworthy that many published population studies have not benefited sufficiently from knowledge on *KIR* polymorphism gained from genomic studies, often reporting only rough analyses of gene content and basic classifications on the “B-ness” or “A-ness” of *KIR* haplotypes.

We have tried to contribute to fill that gap by studying a sample of Spanish individuals by means of: (i) A combination of rapid and advanced methods for *KIR*-gene profiling that inform, not only of presence/absence of *KIR* genes, but also of isoforms associated with defined haplotypes, and recombinants that mark contracted/expanded haplotypes; (ii) Parsimonious interpretation of *KIR*-gene profiles based on accumulated knowledge on common and well-defined haplotypes and alleles; and (iii) Basic molecular characterization of a minority of *KIR*-gene profiles not fitting with known arrangements. Limitations of our study are that polymorphism has, in general, not been defined at an allelic level; and that our parsimonious approach might theoretically overlook part of the existing diversity. To mitigate the latter limitation we have screened certain specific recombinations in donors with compatible profiles, thus identifying individuals in whom variant structures were concealed by the accompanying genes.

By applying systematically this approach, we have managed to explain all 38 gene profiles found in 414 individuals, inferring their haplotype structures and incorporating them to analysis of *KIR*-gene distribution. We have thus determined the detailed distribution of the three fixed centromeric and three telomeric motifs; of six expanded or contracted *KIR*-gene

arrangements characterized previously by us and others, seen in 22 individuals (5.31%); and two novel haplotypes never detected before in Caucasoids. These novel arrangements are associated with new *KIR* alleles, and they show combined features of B- and A-haplotypes.

Transcribed *KIR2DL5B*002* alleles, contrasting with common silent ones, were found within a *2DL5B-2DS3* cluster inserted in a centromeric *2DL3-2DP1-2DL1* motif, thus converting it in a cen-B haplotype. Such structure had been previously reported in individuals of African origin (8, 9, 32). Transcription of *KIR2DL5B*0020106* and **0020202* provides further confirmation to our hypothesis that an intact RUNX binding site in the proximal promoter is essential for *KIR*-gene expression, whilst its mutation determines epigenetic silencing. The biological significance of transcribed *KIR2DL5B*002* alleles is, however, uncertain since, like *KIR2DL5A*005* (Figure 7), the encoded receptor appears not to reach the cell surface and is possibly retained intracellularly (56). The fact that nearly identical coding sequences are preceded by three highly divergent promoter sequences in alleles of two paralog genes (*2DL5A*005*, *2DL5B*0020101* and *2DL5B*0020106/0020202*) illustrates the role of recombination in *KIR*-gene evolution.

The second novel allele, *KIR2DL3*033*, and its associated haplotype do not fit comfortably with the current classification and designation of *KIR* genes and haplotypes, posing a puzzling nomenclature issue. Its long inhibitory tail, homologous to that of common *KIR2DL3* alleles, should warrant its designation as a *KIR2DL*. Such name, however, challenges an unwritten rule of assigning hybrid *KIR* to the locus contributing the extracellular portion (e.g. *2DS2*005*, a *2DS2/2DS3* hybrid, or *3DL1*060*, a *3DL1/3DL2* chimera), and it obviates that most of the gene (~11 of 14 Kbp) and of the encoded molecule (all the ectodomain) are actually identical to those of *KIR2DS2*, and will be detected as such by most current genotyping and phenotyping assays. This may result in ambiguous or conflicting profiles, which can be sorted out by assays that, like the one we have used (Figure 6A), target specifically the *KIR2DL3*033* recombination spot in intron 6. Furthermore, whereas recombinations of B- and A-haplotypes normally yield B-haplotypes, gene content of the hybrid haplotype bearing *2DL3*033* adjusts to the definition of A-haplotypes, its “B-ness” being perceived only when the actual sequence of its centromeric genes (*KIR 3DL3* and *2DL3*) is considered. On the other hand, assigning the new structure to the *KIR2DS2* gene would better reflect its origin, but would imply designating a long-tailed *KIR* with an “S” symbol aimed at distinguishing short-tailed, activating, *KIR*. To circumvent such and similar inconsistencies, the official *KIR* nomenclature might consider in the future the use of dedicated names to describe the hybrid nature of recombinant *KIR* genes (e.g., *KIR2DS2/L3*, *KIR3DL1/L2*, et cetera).

In summary, we consider that our study provides a representative and precise estimate of the *KIR* structures seen in

the Spanish population, and extends our understanding of their complexity in South European Caucasoids. We expect that our results, and the approach we followed to obtain them, will enable better-founded studies of *KIR* in populations, and in health conditions in which their genetic diversity is deemed relevant.

DATA AVAILABILITY STATEMENT

The datasets generated for this study can be found in the EMBL/GenBank/DDBJ HG931348, LT604077.

ETHICS STATEMENT

The studies involving human participants were reviewed and approved by Comité Ético de Investigación con Medicamentos, Hospital Universitario Puerta de Hierro, Majadahonda. The patients/participants provided their written informed consent to participate in this study.

AUTHOR CONTRIBUTIONS

EC designed and performed experiments, analyzed and interpreted data, and wrote the manuscript. MM performed experiments, analyzed and interpreted data, and revised the manuscript. NG-L, AM, and ML-B contributed samples, and revised the manuscript. CV designed the study, directed research and wrote the manuscript.

FUNDING

This work was supported by grants SAF2016-80363-C2-1/2-R (Spanish Ministry of Economy and Competitiveness (MINECO)-FEDER, EU), and PCIN-2015-191-C02-02 (FP7-MINECO Infect-ERA program) to CV and ML-B. MM was supported by *Fundación Asociación Española Contra el Cáncer* (AECC) grant GCB15152947MELE. EC was supported, successively, by grants SAF2010-22153-C03, *Fundació La Marató de TV3* 121531, and PCIN-2015-191-C02-02. AM was supported by Instituto de Salud Carlos III (ISCIII)/FEDER grant PI19/00328. CV was supported in 2019 and 2020 by the nominative grant from *Consejería de Sanidad de la Comunidad de Madrid* to *Fundación de Investigación Biomédica Puerta de Hierro*.

ACKNOWLEDGMENTS

We thank all individuals who generously donated samples for this study. We also thank Dr. Rosario de Pablo, Rosario Solís, and Esperanza Rodríguez (former members of the HLA lab, Inmunología, Hospital Universitario Puerta de Hierro), Gemma Heredia (University Pompeu Fabra), and members of the central facilities of *Instituto de Investigación Sanitaria Puerta de Hierro Segovia de Arana*, for expert support.

REFERENCES

- Vilches C, Parham P. KIR: diverse, rapidly evolving receptors of innate and adaptive immunity. *Annu Rev Immunol.* (2002) 20:217–51. doi: 10.1146/annurev.immunol.20.092501.134942
- Falco M, Pende D, Munari E, Vacca P, Mingari MC, Moretta L. Natural killer cells: from surface receptors to the cure of high-risk leukemia (Ceppellini Lecture). *HLA.* (2019) 93:185–94. doi: 10.1111/tan.13509
- Wroblewski EE, Parham P, Guethlein LA. Two to tango: co-evolution of hominid natural killer cell receptors and MHC. *Front Immunol.* (2019) 10:177. doi: 10.3389/fimmu.2019.00177
- Wilson MJ, Torkar M, Haude A, Milne S, Jones T, Sheer D, et al. Plasticity in the organization and sequences of human KIR/ILT gene families. *Proc Natl Acad Sci USA.* (2000) 97:4778–4783. doi: 10.1073/pnas.080588597
- Sambrook JG, Bashirova A, Andersen H, Piatak M, Vernikos GS, Coggill P, et al. Identification of the ancestral killer immunoglobulin-like receptor gene in primates. *BMC Genomics.* (2006) 7:209. doi: 10.1186/1471-2164-7-209
- Martin AM, Freitas EM, Witt CS, Christiansen FT. The genomic organization and evolution of the natural killer immunoglobulin-like receptor (KIR) gene cluster. *Immunogenetics.* (2000) 51:268–80. doi: 10.1007/s002510050620
- Hsu KC, Chida S, Geraghty DE, Dupont B. The killer cell immunoglobulin-like receptor (KIR) genomic region: gene-order, haplotypes and allelic polymorphism. *Immunol Rev.* (2002) 190:40–52. doi: 10.1034/j.1600-065X.2002.19004.x
- Pyo CW, Guethlein LA, Vu Q, Wang R, Abi-Rached L, Norman PJ, et al. Different patterns of evolution in the centromeric and telomeric regions of group A and B haplotypes of the human killer cell Ig-like receptor locus. *PLoS ONE.* (2010) 5:e15115. doi: 10.1371/journal.pone.0015115
- Pyo CW, Wang R, Vu Q, Cereb N, Yang SY, Duh FM, et al. Recombinant structures expand and contract inter and intragenic diversification at the KIR locus. *BMC Genomics.* (2013) 14:89. doi: 10.1186/1471-2164-14-89
- Roe D, Vierra-Green C, Pyo CW, Eng K, Hall R, Kuang R, et al. Revealing complete complex KIR haplotypes phased by long-read sequencing technology. *Genes Immun.* (2017) 18:127–34. doi: 10.1038/gene.2017.10
- Uhrberg M, Valiante NM, Shum BP, Shilling HG, Lienert-Weidenbach K, Corliss B, et al. Human diversity in killer cell inhibitory receptor genes. *Immunity.* (1997) 7:753–63. doi: 10.1016/S1074-7613(00)80394-5
- Vilches C, Rajalingam R, Uhrberg M, Gardiner CM, Young NT, and Parham P. KIR2DL5, a novel killer-cell receptor with a D0-D2 configuration of Ig-like domains. *J Immunol.* (2000) 164:5797–804. doi: 10.4049/jimmunol.164.11.5797
- Marsh SG, Parham P, Dupont B, Geraghty DE, Trowsdale J, Middleton D, et al. Killer-cell immunoglobulin-like receptor (KIR) nomenclature report, 2002. *Tissue Antigens.* (2003) 62:79–86. doi: 10.1034/j.1399-0039.2003.00072.x
- Maxwell LD, Wallace A, Middleton D, Curran MD. A common KIR2DS4 deletion variant in the human that predicts a soluble KIR molecule analogous to the KIR1D molecule observed in the rhesus monkey. *Tissue Antigens.* (2002) 60:254–8. doi: 10.1034/j.1399-0039.2002.600307.x
- Cisneros E, Moraru M, Gomez-Lozano N, Lopez-Botet M, Vilches C. KIR2DL5: an orphan inhibitory receptor displaying complex patterns of polymorphism and expression. *Front Immunol.* (2012) 3:289. doi: 10.3389/fimmu.2012.00289
- Parham P, Guethlein LA. Genetics of natural killer cells in human health, disease, and survival. *Annu Rev Immunol.* (2018) 36:519–48. doi: 10.1146/annurev-immunol-042617-053149
- Ordóñez D, Meenagh A, Gómez-Lozano N, Castaño J, Middleton D, Vilches C. Duplication, mutation and recombination of the human orphan gene KIR2DS3 contribute to the diversity of KIR haplotypes. *Genes Immun.* (2008) 9:431–7. doi: 10.1038/gene.2008.34
- Gómez-Lozano N, Gardiner CM, Parham P, Vilches C. Some human KIR haplotypes contain two KIR2DL5 genes: KIR2DL5A and KIR2DL5B. *Immunogenetics.* (2002) 54:314–9. doi: 10.1007/s00251-002-0476-2
- Norman PJ, Carrington CV, Byng M, Maxwell LD, Curran MD, Stephens HA, et al. Natural killer cell immunoglobulin-like receptor (KIR) locus profiles in African and South Asian populations. *Genes Immun.* 3:86–95. doi: 10.1038/sj.gene.6363836
- Gomez-Lozano N, de Pablo R, Puente S, and Vilches C. (2003). Recognition of HLA-G by the NK cell receptor KIR2DL4 is not essential for human reproduction. *Eur J Immunol.* 33:639–44. doi: 10.1002/eji.200323741
- Martin MP, Bashirova A, Traherne J, Trowsdale J, Carrington M. Cutting edge: expansion of the KIR locus by unequal crossing over. *J Immunol.* (2003) 171:2192–5. doi: 10.4049/jimmunol.171.5.2192
- Gomez-Lozano N, Estefania E, Williams F, Halfpenny I, Middleton D, Solis R, et al. The silent KIR3DP1 gene (CD158c) is transcribed and might encode a secreted receptor in a minority of humans, in whom the KIR3DP1, KIR2DL4 and KIR3DL1/KIR3DS1 genes are duplicated. *Eur J Immunol.* (2005) 35:16–24. doi: 10.1002/eji.200425493
- Traherne JA, Martin M, Ward R, Ohashi M, Pellett F, Gladman D, et al. Mechanisms of copy number variation and hybrid gene formation in the KIR immune gene complex. *Hum Mol Genet.* (2010) 19:737–51. doi: 10.1093/hmg/ddp538
- Hou L, Chen M, Ng J, Hurley CK. Conserved KIR allele-level haplotypes are altered by microvariation in individuals with European ancestry. *Genes Immun.* (2012) 13:47–58. doi: 10.1038/gene.2011.52
- Valiante NM, Uhrberg M, Shilling HG, Lienert-Weidenbach K, Arnett KL, D'Andrea A, et al. Functionally and structurally distinct NK cell receptor repertoires in the peripheral blood of two human donors. *Immunity.* (1997) 7:739–51. doi: 10.1016/S1074-7613(00)80393-3
- Vilches C, Gardiner CM, Parham P. Gene structure and promoter variation of expressed and non-expressed variants of the KIR2DL5 gene. *J Immunol.* (2000) 165:6416–21. doi: 10.4049/jimmunol.165.11.6416
- Martin MP, Single RM, Wilson MJ, Trowsdale J, Carrington M. KIR haplotypes defined by segregation analysis in 59 Centre d'Etude Polymorphisme Humain (CEPH) families. *Immunogenetics.* (2008) 60:767–74. doi: 10.1007/s00251-008-0334-y
- Selvaraj S, Schmitt AD, Dixon JR, Ren B. Complete haplotype phasing of the MHC and KIR loci with targeted HaploSeq. *BMC Genomics.* (2015) 16:900. doi: 10.1186/s12864-015-1949-7
- Norman PJ, Hollenbach JA, Nemat-Gorgani N, Marin WM, Norberg SJ, Ashouri E, et al. Defining KIR and HLA class I genotypes at highest resolution via high-throughput sequencing. *Am J Hum Genet.* (2016) 99:375–91. doi: 10.1016/j.ajhg.2016.06.023
- Meenagh A, Williams F, Slear C, Halfpenny IA, Middleton D. Investigation of killer cell immunoglobulin-like receptor gene diversity V. KIR3DL2. *Tissue Antigens.* (2004) 64:226–34. doi: 10.1111/j.1399-0039.2004.00272.x
- Middleton D, Meenagh A, Gourraud PA. KIR haplotype content at the allele level in 77 Northern Irish families. *Immunogenetics.* (2007) 59:145–58. doi: 10.1007/s00251-006-0181-7
- Hou L, Chen M, Jiang B, Wu D, Ng J, Hurley CK. Thirty allele-level haplotypes centered around KIR2DL5 define the diversity in an African American population. *Immunogenetics.* (2010) 62:491–8. doi: 10.1007/s00251-010-0458-8
- Hollenbach JA, Nocedal I, Ladner MB, Single RM, Trachtenberg EA. Killer cell immunoglobulin-like receptor (KIR) gene content variation in the HGDP-CEPH populations. *Immunogenetics.* (2012) 64:719–37. doi: 10.1007/s00251-012-0629-x
- Jiang W, Johnson C, Jayaraman J, Simecek N, Noble J, Moffatt MF, et al. Copy number variation leads to considerable diversity for B but not A haplotypes of the human KIR genes encoding NK cell receptors. *Genome Res.* (2012) 22:1845–54. doi: 10.1101/gr.137976.112
- Vierra-Green C, Roe D, Hou L, Hurley CK, Rajalingam R, Reed E, et al. Allele-level haplotype frequencies and pairwise linkage disequilibrium for 14 KIR loci in 506 European-American individuals. *PLoS ONE.* (2012) 7:e47491. doi: 10.1371/journal.pone.0047491
- Pontikos N, Smyth DJ, Schuilenburg H, Howson JM, Walker NM, Burren OS, et al. A hybrid qPCR/SNP array approach allows cost efficient assessment of KIR gene copy numbers in large samples. *BMC Genomics.* (2014) 15:274. doi: 10.1186/1471-2164-15-274
- Roberts CH, Jiang W, Jayaraman J, Trowsdale J, Holland MJ, Traherne JA. Killer-cell Immunoglobulin-like Receptor gene linkage and copy number variation analysis by droplet digital PCR. *Genome Med.* (2014) 6:20. doi: 10.1186/gm537
- Jiang W, Johnson C, Simecek N, Lopez-Alvarez MR, Di D, Trowsdale J, et al. qKAT: a high-throughput qPCR method for KIR gene copy

- number and haplotype determination. *Genome Med.* (2016) 8:99. doi: 10.1186/s13073-016-0358-0
39. Wagner I, Schefzyk D, Pruschke J, Schofl G, Schone B, Gruber N, et al. Allele-level KIR genotyping of more than a million samples: workflow, algorithm, and observations. *Front Immunol.* (2018) 9:2843. doi: 10.3389/fimmu.2018.02843
 40. Gonzalez-Galarza FF, Takeshita LY, Santos EJ, Kempson F, Maia MH, da Silva AL, et al. Allele frequency net 2015 update: new features for HLA epitopes, KIR and disease and HLA adverse drug reaction associations. *Nucleic Acids Res.* (2015). 43:D784–8. doi: 10.1093/nar/gku1166
 41. Gómez-Lozano N, Trompeter HI, de Pablo R, Estefanía E, Uhrberg M, Vilches C. Epigenetic silencing of potentially functional KIR2DL5 alleles: implications for the acquisition of KIR repertoires by NK cells. *Eur J Immunol.* (2007) 37:1954–65. doi: 10.1002/eji.200737277
 42. Vilches C, Castano J, Gomez-Lozano N, Estefanía E. Facilitation of KIR genotyping by a PCR-SSP method that amplifies short DNA fragments. *Tissue Antigens.* (2007) 70:415–22. doi: 10.1111/j.1399-0039.2007.00923.x
 43. Ordóñez D, Gómez-Lozano N, Rosales L, Vilches C. Molecular characterisation of KIR2DS2*005, a fusion gene associated with a shortened KIR haplotype. *Genes Immunity.* (2011) 12:544–51. doi: 10.1038/gene.2011.35
 44. Artavanis-Tsakonas K, Eleme K, McQueen KL, Cheng NW, Parham P, Davis DM, et al. Activation of a subset of human NK cells upon contact with *Plasmodium falciparum*-infected erythrocytes. *J Immunol.* (2003) 171:5396–405. doi: 10.4049/jimmunol.171.10.5396
 45. Norman PJ, Abi-Rached L, Gendzekhadze K, Hammond JA, Moesta AK, Sharma D, et al. Meiotic recombination generates rich diversity in NK cell receptor genes, alleles, and haplotypes. *Genome Res.* (2009). 19:757–69. doi: 10.1101/gr.085738.108
 46. Stephens M, Smith NJ, Donnelly P. A new statistical method for haplotype reconstruction from population data. *Am J Hum Genet.* (2001) 68:978–89. doi: 10.1086/319501
 47. Stephens M, Donnelly P. A comparison of bayesian methods for haplotype reconstruction from population genotype data. *Am J Hum Genet.* (2003) 73:1162–9. doi: 10.1086/379378
 48. Gaunt TR, Rodriguez S, Day IN. Cubic exact solutions for the estimation of pairwise haplotype frequencies: implications for linkage disequilibrium analyses and a web tool “CubeX.” *BMC Bioinformatics.* (2007) 8:428. doi: 10.1186/1471-2105-8-428
 49. Estefanía E, Flores R, Gómez-Lozano N, Aguilar H, López-Botet M, Vilches C. Human KIR2DL5 is an inhibitory receptor expressed on the surface of NK and T lymphocyte subsets. *J Immunol.* (2007) 178:4402–10. doi: 10.4049/jimmunol.178.7.4402
 50. Leaton LA, Shortt J, Kichula KM, Tao S, Nemat-Gorgani N, Mentzer AJ, et al. Conservation, extensive heterozygosity, and convergence of signaling potential all indicate a critical role for KIR3DL3 in higher primates. *Front Immunol.* (2019) 10:24. doi: 10.3389/fimmu.2019.00024
 51. Diaz-Pena R, Vidal-Castineira JR, Moro-Garcia MA, Alonso-Arias R, Castro-Santos P. Significant association of the KIR2DL3/HLA-C1 genotype with susceptibility to Crohn’s disease. *Hum Immunol.* (2016) 77:104–9. doi: 10.1016/j.humimm.2015.10.020
 52. Castano-Nunez A, Montes-Cano MA, Garcia-Lozano JR, Ortego-Centeno N, Garcia-Hernandez FJ, Espinosa G, et al. Association of functional polymorphisms of KIR3DL1/DS1 with Behcet’s disease. *Front Immunol.* (2019) 10:2755. doi: 10.3389/fimmu.2019.02755
 53. Closa L, Vidal F, Herrero MJ, Caro JL. Distribution of human killer cell immunoglobulin-like receptors and ligands among blood donors of Catalonia. *HLA.* (2019) 95:179–88. doi: 10.1111/tan.13754
 54. Bono M, Pende D, Bertaina A, Moretta A, Della Chiesa M, Sivori S, et al. Analysis of KIR3DP1 polymorphism provides relevant information on centromeric KIR gene content. *J Immunol.* (2018) 201:1460–7. doi: 10.4049/jimmunol.1800564
 55. Nakimuli A, Chazara O, Farrell L, Hiby SE, Tukwasibwe S, Knee O, et al. Killer cell immunoglobulin-like receptor (KIR) genes and their HLA-C ligands in a Ugandan population. *Immunogenetics.* (2013) 65:765–75. doi: 10.1007/s00251-013-0724-7
 56. Cisneros E, Estefanía E, Vilches C. Allelic polymorphism determines surface expression or intracellular retention of the human NK cell receptor KIR2DL5A (CD158f). *Front Immunol.* (2017) 7:698. doi: 10.3389/fimmu.2016.00698
- Conflict of Interest:** The authors declare that the research was conducted in the absence of any commercial or financial relationships that could be construed as a potential conflict of interest.
- Copyright © 2020 Cisneros, Moraru, Gómez-Lozano, Muntasell, López-Botet and Vilches. This is an open-access article distributed under the terms of the Creative Commons Attribution License (CC BY). The use, distribution or reproduction in other forums is permitted, provided the original author(s) and the copyright owner(s) are credited and that the original publication in this journal is cited, in accordance with accepted academic practice. No use, distribution or reproduction is permitted which does not comply with these terms.